

Complexing capacity profiles of naturally occurring ligands in Tempranillo wines for Cu and Zn. An electroanalytical approach for cupric casse.

I. Esparza^a, C. Santamaría^a, J.M. García-Mina^b, J.M. Fernández^a

^a Departamento de Química y Edafología, Universidad de Navarra, c/. Irunlarrea 1, 31080 Pamplona, Navarra, Spain

^b INABONOS, Polígono Arazuri, 31160 Orcoyen, Navarra, Spain

Abstract

Complexing capacity of naturally occurring ligands in *Vitis vinifera* (Tempranillo variety) wines has been studied with respect to two target metals (Cu and Zn) by Differential Pulse Anodic Stripping Voltammetry (DPASV). Eight commercial wines of two certified brands of origin (CBO) and a young wine along its vinification process were monitored. Conditional stability constants and total complexing ligand(s) concentration have been calculated for both metals. Discussion of the particular electrochemical response for Cu and Zn for all samples is presented. A follow-up of the Cu stripping response allowed differentiating a commercial wine from one under processing related to the cupric casse phenomenon. Interaction of Cu with two molecular forms of cyanidin has been theoretically modeled at natural wine pH.

Keywords

Complexation; wine; vinification; Cu; Zn; cupric casse; Differential Pulse Anodic Stripping Voltammetry (DPASV)

Introduction

Amongst all beverages and drinks, wine has always been the favourite for human consumption for centuries. Beneficial properties have been associated with its constituents, and nowadays cardiovascular protector and antioxidant roles are much spread and appreciated [1]. These characteristics have been definitely related to the organic fraction, i.e. anthocyanins and tannins, and accordingly a good number of papers have been released in which wine composition has been analysed for different varieties, origins and viticulture practices [2-5]. Metals present in the wine matrix play a substantial role as yeast cofactor [6], oligoelements [7] metallic targets for complexes [8], and fingerprints of geographical origin of wine [9]. Oenological attention devoted to metals has been extensively centred on the ferric and cupric cases [10], and the possible toxicity of certain heavy metals arising from the cultivation area and its environment [11-12]. Usually, research has been focused in either the organic or the inorganic fraction, while the integral study of all constituents has scarcely been done.

Zn and Cu have both been chromatographically found to specifically associate to cyanidin-3-glucoside which is one of the most abundant anthocyanins in red wines [13] and their complexing capability with individual polyphenols in different media has been electrochemically evaluated [14-17]. Presence of metals accompanying natural ligands in commercial wines comes as a result of their mutual interaction along winemaking where metals intervene in multiple processes such as complex formation [18], polymerization, flocculation and precipitation [6,10,19]. Besides, Zn concentration remains more or less constant along vinification, while Cu profile shows a decreasing tendency [13,20].

The above described distinct behaviour could be an expression of a different complexing pattern for both metals which we have tried to clarify through their well

known electrochemical stripping response. To this aim, a *Vitis vinifera* (Tempranillo variety) wine has been thoroughly studied along its processing life in experimental conditions that do not alter the naturally occurring equilibria in this heterogeneous matrix; its complexing ability with respect to the two selected metals, ligand population concentration, stereochemistry and stoichiometry have been evaluated. Several commercial wines have been treated in a similar way as to check whether a differentiation could be found between wine under vinification and bottled wine in terms of their electrochemically calculated complexing parameters.

Experimental

Wine samples

Studies have been carried out from *Vitis vinifera* (Tempranillo variety) grapes collected in the 2004 campaign at an experimental vineyard located in Olite (Navarra) supervised by EVENA. Sampling was done up to the moment of transfer onto the oak barrel. For the first eleven days, samples were taken daily; henceforth, collection was restricted to days 18, 25, 32, 51 and 58 of vinification.

Commercial Tempranillo variety wines from two different certified origins (Navarra –N1 to N6- and La Rioja –R1 and R2-) and assorted harvests (2001 to 2004) were also studied.

Sample preparation

Since the calculation of ligand population and the estimation of conditional constant values requires the total metal concentration to be known, samples have been microwave-digested with sub-boiling nitric acid, by using an Ethos Plus computer-controlled model provided with the easyware® software. Commercial wines were microwaved as such, whereas samples under vinification were previously centrifuged in order to separate dregs from supernatants by using a Biofuge Stratus (Heraeus) centrifuge, at 4°C ; 6 mL sub boiling (s.b.) HNO₃ was added to each 2 mL supernatant sample before proceeding to the microwave assisted digestion routine, that was identical to that published elsewhere [13]. Once digested, all samples were taken to 10 mL volume with ultra-pure water. In all instances, samples were processed by triplicate.

Quantification of Cu and Zn

A Perkin Elmer Atomic Absorption Spectrometer A Analyst 800, was used with an air-acetylene flame under these conditions:

Metal	λ (nm)	Slit	Lamp current (mA)	Calibration interval	Calibration line	*Detection limit	*Quantification limit
Zn	213.9	0.7	15	0–0.3 mg L ⁻¹	$y = 0.307x + 1.86 \cdot 10^{-3}$	0.0018 mg L ⁻¹	0.006 mg L ⁻¹
Cu	324.8	0.7	15	0–0.6 mg L ⁻¹	$y = 0.0764 x + 1.43 \cdot 10^{-4}$	0.007 mg L ⁻¹	0.025 mg L ⁻¹

*Detection and quantification limits according to the classical procedure [21].

Electrochemical studies of Cu and Zn

Stock standard solutions of 2.0 and 2.5 ppm were prepared for Cu and Zn, respectively, in a pH 4 acetate buffer with 8% ethanol, from Merck certipure 1000 ppm solutions.

Final commercial wines are subjected to a 10-fold dilution with the same buffer prior to transfer into the electrochemical cell. For wines under vinification, only supernatants are considered. Titration consisted on successive 50 μ L additions of either standard solution. Differential Pulse Anodic Stripping Voltammetry (DPASV) measurements were carried out in an Autolab PGSTAT 12 (EcoChemie) coupled to a Metrohm 663VA Stand under the specified conditions:

	Cu	Zn
Drop size	3	3
Purge time (s)	300	300
Conditioning time (s)	180	1800

Rotation speed (rpm)	3000	3000
Accumulation potential (E_{acc} , V)	-0.600	-1.200
Accumulation time (s)	60	60
Equilibration time (s)	20	20
Initial potential (V)	-0.600	-1.200
Final potential (V)	0.300	-0.200
Pulse amplitude (mV)	50	70
Scan speed ($mV s^{-1}$)	25	20

Data treatment

Titration data were processed according to both Scatchard [22] and Langmuir [23] linearization algorithms. This methodology has been applied to wine matrices before and has been published elsewhere [24]. Equations arising from these mathematical treatments are:

$$[ML]/[M'] = K' [L_T] - k' [ML] \quad \text{and} \quad [M']/[ML] = [M']/[L_T] + 1/K' [L_T], \quad \text{respectively,}$$

where $[M']$ is the free metal concentration; $[ML]$ stands for the complexed metal concentration obtained by subtracting $[M']$ from the total metal concentration $[M_T]$; $[L_T]$ is the total ligand concentration as calculated from these expressions and, finally, K' is the conditional stability constant derived from the slope and from the ordinate of the respective plots.

Theoretical complexation studies for polyphenols with Cu

A theoretical study of the chemical interaction between the major polyphenols present in red wine and Cu has been done in a pH 4-acetate buffer. The operational and theoretical approaches were made assuming that, in general, inter-molecular chemical interactions have two main, successive, steps:

First, a spatial approaching of the interacting molecules that is governed by electrostatic forces related to the electric charge distribution (atomic charges) on each molecule (the inter-molecular approaching interaction is of an electrostatic nature). This first step was studied through the energy minimization of the chemical system using molecular mechanics. Both MM+ [25] and Amber force fields [26] were used, and the geometry and the atomic charges of the individual molecules were previously obtained using a semi-empirical quantum mechanics method PM3 [27].

Second, the chemical interaction between specific regions of the molecules that have achieved the bond distance as a consequence of the inter-molecular approaching interaction, with the creation of new chemical bonds (binding interaction) and we studied the formation of stable binding interactions (that is to say, the creation of new chemical bonds) between those regions of the molecules that have achieved the bond distance as the consequence of the inter-molecular approaching interaction (electrostatic interaction). To this end, we carried out the energy minimization of the chemical systems obtained from the electrostatic interaction, using the semi-empirical method Zindo/1 [28] quantum mechanics.

Throughout the theoretical study we assume that considered polyphenols are uncharged at acid pH (phenols not ionized) except in the case of the anthocyanidin that was calculated with charge +1. Likewise, we consider the $Cu (H_2O)_6^{2+}$ ion, and a 1:1 stoichiometry. Calculations were carried out by means of Hyperchem® 7.0

3. RESULTS AND DISCUSSION

3.1 Electrochemical study of Zn

DPASV was the electrochemical technique chosen to study the behavior of wine samples after the addition of increasing amounts of Zn. Figure 1 shows examples of some of the voltammetric responses recorded for selected samples, when they were spiked with the Zn standard solution. Figures 1a and 1b, correspond to wine samples obtained after short fermentation times. Both samples present a continuous cathodic shift in the peak potential during the first twelve standard spikes. After addition number twelve, peak potential stabilizes in both cases. Wine samples corresponding to longer fermentation times (Figure 1c) do not show any peak potential shift and all the studied samples whose voltammograms are not shown, did follow the same pattern.

One of the most surprising features observed during the performance of these experiments was the fact that, when mercury drops were dislodged from the electrode, each and everyone of them remained isolated from the rest at the bottom of the cell. Such behavior is most likely due to surface adsorption of either one or several polyphenolic and/or anthocyanic compounds present in wine, preventing the mercury drops to collapse together –as usual- in a bigger drop. The adsorption process takes place almost instantaneously, as soon as the mercury drops contacts the wine solution, whatever the wine sample studied.

However, adsorption of polyphenols and/or anthocyanins onto the mercury surface also affects the electrochemical response of the sample, as has been shown by the "evolution" of the voltammograms with increasing added Zn concentrations (Figure 1a and 1b). Re-oxidation of amalgamated Zn from the modified mercury surface seems to be easier as Zn concentration increases, since the oxidation peak shifts towards more negative values. Organic hydrophobic molecules emerging in short time fermented wine could be responsible for these adsorption phenomena. Such molecules appear to complex Zn quite strongly, when the metal is at low concentrations but the strength of the association decreases, on average, as Zn concentration increases.

Wine samples collected at longer fermentation times (Figure 1c) and commercial wines (Figure 1d) did show but a constant potential peak which height increased with increasing Zn concentrations, for all the voltammograms recorded thereafter (even those not shown).

A large variety of chemical transformations take place along wine fermentation, so that concentration of most components of this complex matrix is affected. As a matter of fact, a rapid increase in polyphenols and anthocyanins concentration was found in the early three or four days of fermentation as reported elsewhere for wine prepared from same variety grapes collected at the same spot in the previous vintage (2002), reaching a plateau for longer fermentation days [13]. Thus, DPASV appears to be an efficient and extremely sensitive tool to detect the diverse complexing-adsorption patterns onto the mercury electrode. Analyzed samples corresponding to very short fermentation periods show a variable potential peak voltammograms (Figure 1a and 1b) whilst -once the polyphenols and anthocyanins content is stabilized- constant peak potential curves are obtained for longer fermentation time samples (Figure 1c).

Logically, original Zn concentration values may differ from one sample to other and from one commercial brand to another, and might be invoked as a cause for observed variations in the voltammograms features; however, a relatively constant Zn concentration has been quantified along vinification in this same vintage (see Table 1 below) as well as in vintage 2002.

Titration data collected for Zn standard additions on both experimental vineyard wines under vinification process and on several commercial wines were processed according to two mathematical algorithms that had firstly been explored for 1:1 stoichiometries of metal complexes on estuary waters [23] and lately on wines [24]. As reflected in Table 1, all of them adjusted fairly well to the proposed stoichiometry showing that, on average, natural ligands present in wine –from the early stages of fermentation up to bottled and commercialized ones- behave as a complexing pool agent on Zn with a dissociable 1:1 complex nature.

3.2 Cu Analysis

3.2.1. Electrochemical Study

Figure 2 shows voltammograms recorded for wine samples collected at different vinification stages as well as for commercial wine samples. Cu stripping peak at ca. 0.160 V is always observed and sometimes preceded by a signal at ca. 0.090 V. The magnitude and relevance of this last signal seem to depend on the condition of the analyzed wine. Thus, for early vinification wines a shoulder is visible even for the original samples before any addition of standard metal is done (Figure 2, a-1). Both signals increase as Cu concentration is made larger in solution, up to a point in which the more anodic peak ceases to grow while the shoulder develops into a well defined peak responsive to Cu concentration in solution (Figure 2, a-2). As vinification proceeds, the shoulder does not develop until a few Cu standard additions are made (Figure 2, b-1); the number of additions required for the shoulder to appear is larger as the vinification process advances (not shown). Finally, samples taken just before introducing wine to the oak barrel, show again a stripping pattern very close to initial one, with a visible shoulder (Figure 2, c-1) that soon afterwards becomes the main increasing peak with Cu concentration (Figure 2, c-2). Both vinification day and original sample copper concentrations can be held responsible for variations found.

Commercial bottled wines yielded voltammograms in which the signal with higher peak potential almost vanished and the less anodic peak is always the predominant stripping signal (Figure 2, d-1 and e-1). This behaviour seems indicative of a different mechanism for Cu re-oxidation from the amalgamated metal on the mercury electrode depending on the composition of the wine matrix. These facts may be ascribed to a lesser presence of adsorbed ligands with the ability to stabilise intermediate Cu(I) species as compared to the samples under vinification. Thus, it is clear that at a certain stage in wine processing -in either barrel or bottle-, the nature and/or complexing capacity of this kind of Cu(I)-stabilising ligands undergo a dramatic change. For example, phenomena such as polyphenols polymerization and tannin-anthocyanin condensation processes are known to take place [10]. The simple recording of a voltammogram of a sample would provide a useful tool to discriminate whether the wine is in its final condition or either still under vinification.

Titration behaviour was further checked by plotting peak intensity from both stripping signals vs. added Cu concentration. Figure 3 shows how the less anodic peak intensity continuously increases with added Cu (a), whilst the more anodic peak intensity bends and eventually reaches a plateau (b). Up to three linear segments may be differentiated in the two graphics that correlates with each other. Batley [29] observed a somewhat similar situation when studying Cu complexation in waters, what was later confirmed by Botelho et al [30]. Their conclusions may be applicable to this situation in which up to three electrochemical processes can be invoked, namely: a straight Cu(Hg)^0 to Cu^{2+} re-oxidation at the less positive potential that overlaps with a Cu(Hg)^0 to Cu^+ stabilised by ligands adsorbed on the electrode surface, and a subsequent Cu^+ to Cu^{2+} that occurs at more positive potentials. Thus when plotting $i_{\text{peak 1}}$ vs added Cu concentration, two initial straight portions are obtained that may account for both coalescent processes in an unknown and probably variable ratio. Nevertheless, when added Cu is in excess with respect to the complexing capacity of adsorbed ligand, a new straight line is obtained with a steeper slope that reflects direct re-oxidation of amalgamated copper to the divalent species. These latter points correspond to the plateau obtained in Figure 3b in which the stripping current of the most anodic signal ceases to grow, what implies that no more adsorbed-ligand-stabilised intermediate Cu^+ is formed. These experimental findings are consistent with the hypothesis above

described, in which the predominant electrochemical process during the first group of Cu additions is re-oxidation from amalgamated copper to intermediate monovalent copper that remains adsorbed as a complex on the surface of the mercury electrode; the second group of additions reflect an increasing stripping intensity for peak 1 and a decreasing intensity for peak 2, indicating that predominant electrochemical process in peak 1 is now the re-oxidation to divalent copper, provoking a corresponding diminishing slope for Figure 3b; this direct Cu(Hg)^0 to Cu^{2+} re-oxidation eventually turns out to be the only one electrochemical process at the less positive potential 0.090 V.

A completely similar titration data pattern has been found for commercial wines, with the singularity that, in all of them, the first linear portion is always shorter than for wines under vinification. No need to say that this circumstance is referred to the titration data collected for the unique signal recorded for commercial wines at the less anodic potential of ca. 0.090 V. These results come to confirm that the data grouped in the first linear segment are due to the Cu(Hg)^0 to adsorbed-ligand-stabilised Cu(I). There exists a direct correlation between the length of this initial linear part of the titration graph and the presence and size of the more anodic peak, that is to say with the concentration of adsorbed ligands able to stabilise Cu(I) species. For wines under vinification, first break of linearity in the titration graph was obtained for values of added Cu ranging from 1.2 to 2.5 μM , while additions of Cu forcing the break in the corresponding titration graph for commercial wines oscillate from 0.6 to 1.1 μM . Furthermore, if we pay attention to commercial wines N1 and N4 (voltammograms showed in Figure 2, d-1 and e-1, respectively) the estimated values for Cu added concentrations in the breaking point are 1.05 and 0.6 μM , respectively, that fairly well correlate with the fact that a slight anodic shoulder appears for N1, that is non-existing for N4.

Once an inward look has been paid to the electrochemical behaviour, the complexing ligand population has been calculated from both Langmuir and Scatchard algorithms, that yielded excellent straight population of data, showing that –on average- present ligand(s) act as a 1:1 complexing agent with respect to Cu (see Figure 4). Results are collected in Table 2 where it can be seen the good agreement of values reached by both methodologies for examined samples, i.e. those under vinification and those bottled ones. Generally, in all commercial wines, the representative picture obtained is that of Figure 2 e-1, in which the more anodic signal does not appear, corroborating that Cu(I)-stabilising ligand population has dramatically diminished. This is in good agreement with the results in Table 2 in which total ligand population -that is to say, those able to stabilise Cu(II) species in solution plus those adsorbed ones able to stabilise Cu(I) intermediate species- for commercial wines are generally lower than those found for any wine under vinification.

On the other hand, if we compare the values corresponding to N1 (1.340) and N4 (0.795), we can observe that total ligand population for N4 is much lower than that for N1 what keeps a direct correspondence with the absence of the more anodic peak in the voltammogram of N4 (Figure 2, e-1), while for N1 the more anodic peak is still slightly visible (Figure 2, d-1) indicative of the availability of very little Cu(I)-stabilising ligand.

All these findings point out to the feasibility of an electrochemical discrimination of a wine under processing from a commercial one. Keeping in mind the chemical processes taking place along vinification, it should be emphasized that proteins are able to both complex with tannins yielding a negative hydrophobic colloid that flocculates in the presence of certain cations, and to undergo denaturation processes that leave -SH groups free to interact with both Cu^+ and Cu^{2+} [10,19]. These phenomena are the base for the cupric casse, that occurs along winemaking.

Accordingly, commercial red wines do not suffer this process since proteins have precipitated before. The presence of the double stripping peak is then related to the proteins and their complexing role for Cu^+ and Cu^{2+} species. As a consequence, complexing capacity of commercial wines with respect to the studied metal can only be ascribed to the presence of polyphenols, whereas in the case of wines under vinification both polyphenols and proteins can be invoked as complexing agents for Cu^{2+} ions, while Cu^+ can only be complexed by proteins through their cysteine moiety.

With respect to conditional stability constants (Table 2), Vasconcelos *et al.* have reported similar values for Cu with natural ligands in wine [18], although their experimental calculations for total ligand concentrations notably differ from our results. In our opinion this is a very remarkable fact, for it shows that affinity of the metal for natural wine ligands is similar in different varieties but concentration of complexing ligand may vary from one to another. On the contrary, differences found within the same variety wines are much smaller, as can be seen in Table 2.

It is noteworthy that complexing population seem to be different from one species to the other, that is to say for Zn and Cu. As a matter of fact, in Table 1 it can be seen that complexing ligand availability increases with vinification time for Zn, while it tends to decrease for Cu. We have to recognise that complexing capability arises from a variety of polyphenols and -in the case of Cu- proteins are involved as well [31]. The continuous disappearing of proteins from solution along vinification accounts for the ligand population decrease for Cu.

On the other hand, calculated conditional stability constants for Cu tend to be larger than those calculated for Zn, and a remarkable agreement is found for values calculated by the two algorithms, independent of either metal or complexing ligand concentrations. This good matching reinforces the idea that a 1:1 stoichiometry is the most likely average of the multiple complexes that may be generated in solution.

As above mentioned, Cu-protein interaction is well documented and admitted as proceeding through the thiol groups of cysteine residues; however, Cu-polyphenols linkage position is not so definitely stated, although several authors have used different techniques to characterise the binding site [16, 32, 33]. This has encouraged us to try and find the most favoured interaction by means of a theoretical model.

3.2.2 Theoretical calculations

We focused our attention on Cu and four molecules: an anthocyanidin (cyanidin), two flavonols (myricetin and quercetin) and a flavonol (catechin). Preliminary studies showed that all of them adjusted fairly well to a 1:1 stoichiometry. Since cyanidin is one of the most abundant polyphenols in wine and -most of all- since it is the only one that was found to closely correlate with metals in the fractionation of a wine sample [13], further attention was paid to its complexing capacity with respect to Cu. Brouillard *et al.* [34] have reported that at pH 4 at least four molecular forms may be found in equilibrium, namely, carbinol (49.4%), chalcone (30.1%), quinone (16.3%) and flavilio form (4.2%); the latter form was not considered given its low percentage at the working pH [35]. Accordingly, we have studied the carbinol, the chalcone (isomer *trans*, that is the most stable isomer) and the quinone structures of cyanidin. The energy minimisation test revealed that only the carbinol (Figure 5, 1) and chalcone (Figure 5, 2) forms generated acceptable optimised structures. Interaction studies of carbinol and chalcone forms with Cu gave rise to findings that may be summarised as follows:

- Carbinol cyanidin-Cu. Favourable electrostatic interactions may proceed through three different pathways: one involving just ring C, other implying coupling with both rings A and B, and another comprising the three rings A, B

and C. As for the binding interaction, most stable situation is achieved for the third one, in which the cyanidin is folded over the Cu ion in which aromatic π electrons from A and C rings are strongly involved (Figure 6).

- *trans*-Calchone cyanidin-Cu. Electrostatic interactions take place either through ring A, or ring C, or B structural moiety (Figure 5, 2). These different interactions were associated with two equivalent-energy binding processes (Figure 7). As it can be seen, aromatic π electrons from C ring, and both aromatic π electrons and the hydroxyl group from ring A are directly involved, as well as the hydroxyl and carbonyl groups present in the B moiety. It is noteworthy that binding takes place not only through the typically invoked hydroxyl and carbonyl groups [36] but rather through the aromatic rings of the molecules, as also reported by Vestergaard *et al.* [16].

4. CONCLUSIONS

Anodic stripping voltammetric signals of Zn and Cu in real wine samples have demonstrated to be suitable tools to: 1) unambiguously identify initial stages of vinification by monitoring the stripping peak of Zn, and 2) discriminate between winemaking samples and bottled wine samples by means of the analytical response of Cu.

Conditional stability constants for Zn and Cu with natural ligands occurring in wine both at different stages along vinification and in commercial wines are calculated by two methodologies; obtained two groups of data showed an excellent agreement from which a 1:1 stoichiometry can be undoubtedly concluded.

Calculated ligand concentrations point to polyphenols as main responsible for Zn complexation, while in the case of Cu proteins seem to be involved as well.

Acknowledgements

Funding was provided by the Department of Education of the Government of Navarra. I. Esparza has benefited a doctoral grant from the Government of Navarra . M. Yárnoz is thanked for her co-operation.

References

- [1] J.B. German, R.L. Walzem, *Annu. Rev. Nutr.*, 20 (2000) 561.
- [2] M. Monagas, C. Gómez-Cordovés, B. Bartolomé, *Food Chem.*, 95 (2006) 405.
- [3] S. Pérez-Magariño, M.L. González-San José, *Food Chem.*, 96 (2006) 197.
- [4] M.A. Cliff, M.C. King, J. Schlosser, *Food Res. Int.*, 40 (2007) 92.
- [5] A. Peña, T. Hernández, C. García Vallejo, I. Estrella, J.A. Suárez, *Eur. Food Res. Technol.*, 210 (2000) 445.
- [6] C.Z. Fernández Pereira, *Z. Lebensm Unters Forsch.*, 186 (1988) 295.
- [7] H. Eschnauer, R. Neeb, in: H.F. Linskens, J.F. Jackson (Eds.), *Microelement analysis in wine and grapes*, Springer-Verlag, Berlin, 1988, p. 67.
- [8] M. Satterfield, J.S. Brodbelt, *Anal. Chem.*, 72 (2000) 5898.
- [9] J.M. González, M.C. Martínez, M.V. Aguilar, *Z. Lebensm Unters Forsch. A*, 187 (1988) 325.
- [10] P. Ribéreau-Gayon, Y. Glories, A. Maujean, D. Dubourdieu, in: *Tratado de enología, 2. Química del vino. Estabilización y tratamientos*, Mundi-Prensa Ediciones, Buenos Aires, Argentina, 2002, p 126.
- [11] G. Scollary, *Analisis*, 25 (1997) M 26.
- [12] M. Aceto, O. Abollino, M.C. Bruzzoniti, E. Mentast, C. Sarzanini, M. Malandrino, *Food Addit. Contam.*, 19 (2002)126.
- [13] I. Esparza, Í. Salinas, I. Caballero, C. Santamaría, I. Calvo, J.M. García-Mina, J.M. Fernández, *Anal. Chim. Acta*, 524 (2004) 215.
- [14] M.E. Bodini, M.A. del Valle, R. Tapia, F. Leighton, P. Berrios, *Polyhedron*, 20 (2001) 1005.
- [15] G. Le Nest, O. Caille, M. Woudstra, S. Roche, B. Burlat, V. Belle, B. Guigliarelli, D. Lexa, *Inorg. Chim. Acta*, 357 (2004) 2027.
- [16] M. Vestergaard, K. Kerman, E. Tamiya, *Anal. Chim. Acta*, 538 (2005) 273.
- [17] I. Esparza, Í. Salinas, C. Santamaría, J.M. García-Mina, J.M. Fernández, *Anal. Chim. Acta*, 543 (2005) 267.
- [18] M.T. Vasconcelos, M. Azenha, V. de Freitas, *J. Agric. Food Chem.*, 47 (1999) 2791.
- [19] L. Usseglio – Tomasset, in: *Química Enológica*, Mundi-prensa, Madrid, Spain, 1998, p 300.
- [20] M.M. Castiñeira, G.R. Brandt, N. Jakubowski, T. Andersson, *J. Agric. Food Chem.*, 52 (2004) 2953.
- [21] D. MacDougall, W.B. Crummett, *Anal. Chem.*, 52 (1980) 2242.
- [22] G. Scatchard, *Ann. N.Y. Acad. Sci.*, 51 (1949) 660.
- [23] C.M.G. van den Berg, J.R. Kramer, *Anal. Chim. Acta*, 106 (1979) 113.
- [24] Í. Salinas, I. Esparza, S. Gómez, C. Santamaría, J.M. Fernández, *Electroanalysis*, 17 (2005) 469.
- [25] N. Allinger, *J. Am. Chem. Soc.*, 99 (1997) 8127.
- [26] S.J. Weiner, P.A. Kollman, D.A. Case, U.C. Singh, C. Ghio, G. Alagona, S. Profeta, P. Weiner, *J. Am. Chem. Soc.*, 106 (1984) 765.
- [27] J.J. Stewart, *J. Comput. Chem.*, 10 (1989) 209.
- [28] W.D. Edwards, M.C. Zerner, *Theoret. Chim. Acta*, 72 (1987) 347.
- [29] G. E. Batley, *Anal. Chim. Acta*, 189 (1986) 371.
- [30] C.M.S. Botelho, R.A.R. Boaventura, M.L.S. Simões Gonçalves, *Electroanalysis*, 14 (2002) 1713.
- [31] I. Karadjova, B. Izgi, S. Gucer, *Spectrochim. Acta B*, 57 (2002) 581.
- [32] A. Torreggiani, M. Tamba, A. Trincherro, S. Bonora, *J. Mol. Struct.*, 744–747 (2005) 759.
- [33] M. Satterfield, J.S. Brodbelt, *Anal. Chem.*, 72 (2000) 5898.
- [34] R. Brouillard, B. Delaporte, J.E. Dubois, *J. Am. Chem. Soc.*, 100 (1978) 6202.
- [35] Y. Glories, *Conn. Vigne. Vin.*, 18 (1984) 253.
- [36] J.E. Brown, H. Khodr, R.C. Hider, C.A. Rice-Evans, *Biochem. J.*, 330 (1998) 1173.

Figure 1. Voltammograms recorded along titration with Zn in wines under vinification (a: day 1; b: day 2; c: day 58) and in a commercial wine (d: N1, 2001 vintage). $E_{acc} = -1.200$ V

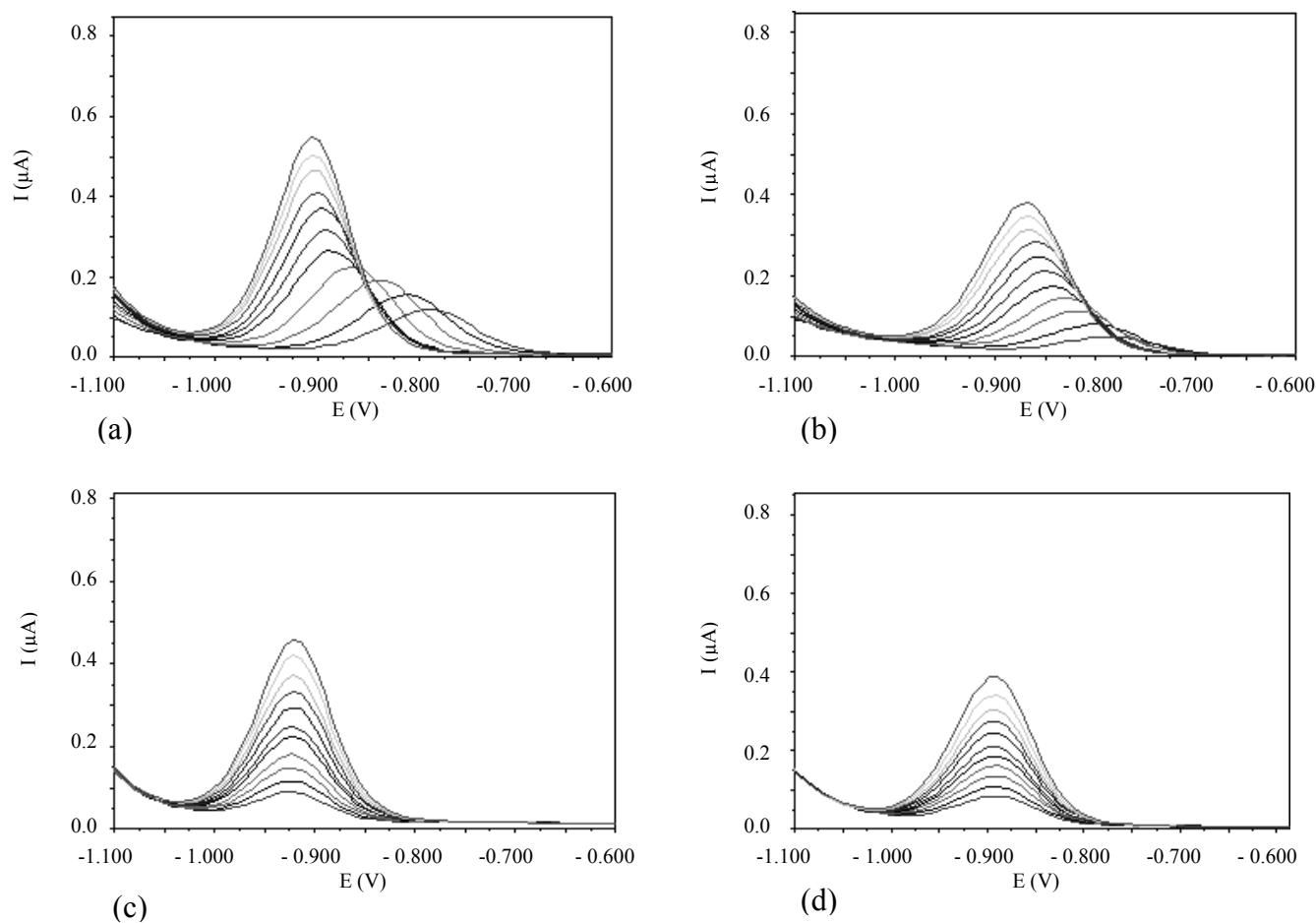


Figure 2. Voltammograms obtained along titration with Cu in wines under vinification process (a: day 1; b: day 6; c: day 58) and in commercial wines (d: N1, 2001 vintage; e: N4, 2004 vintage). $E_{acc} = -0.600$ V
a-1, b-1, c-1, d-1 and e-1: base line and first 10 spikes of standard Cu; a-2, b-2, and c-2: following 11 additions.

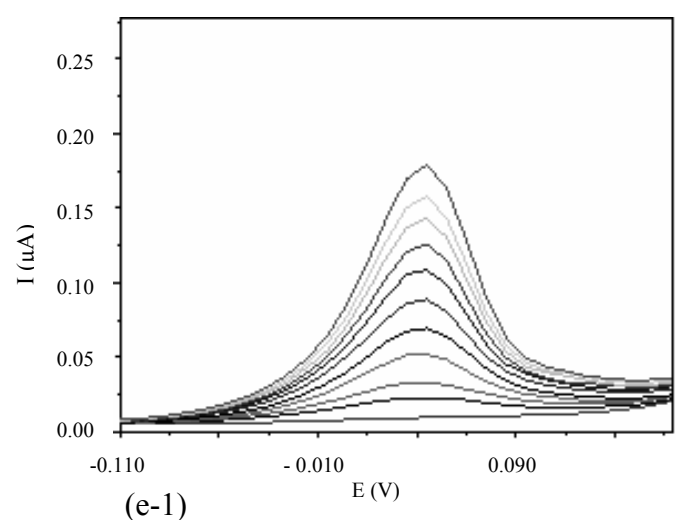
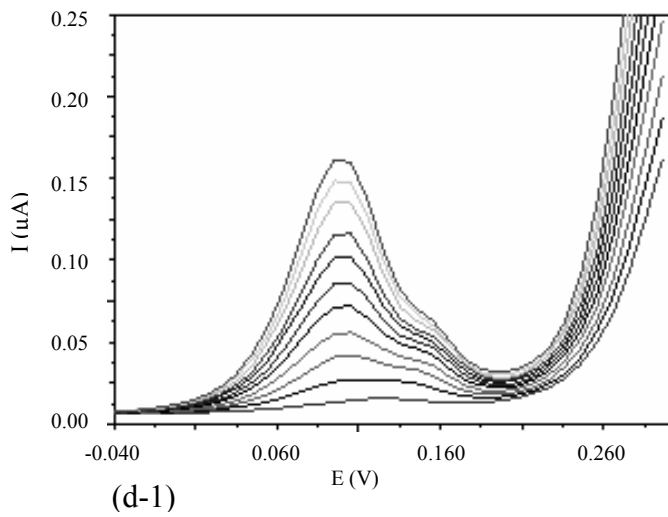
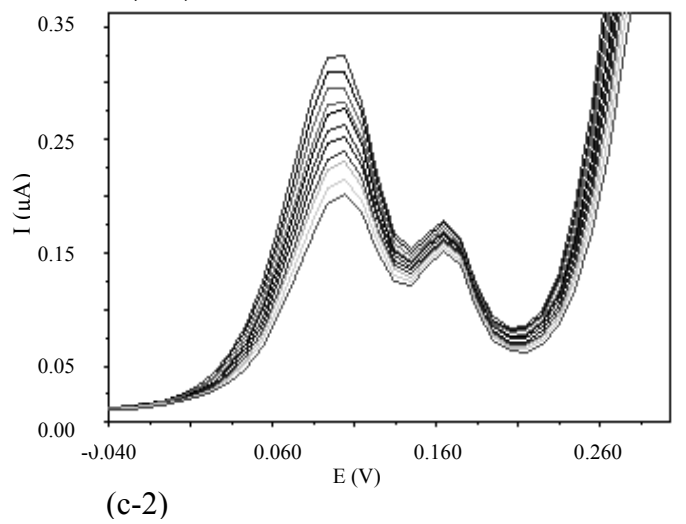
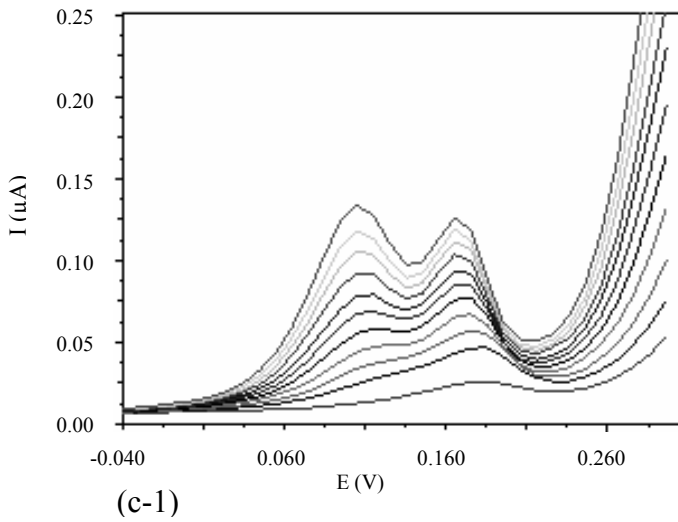
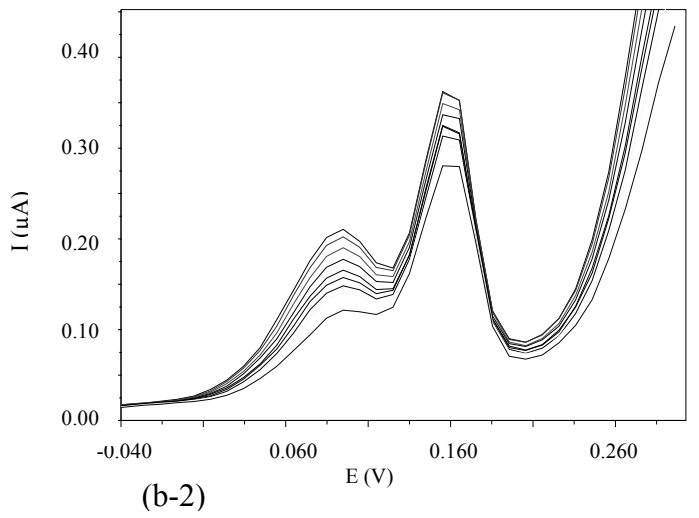
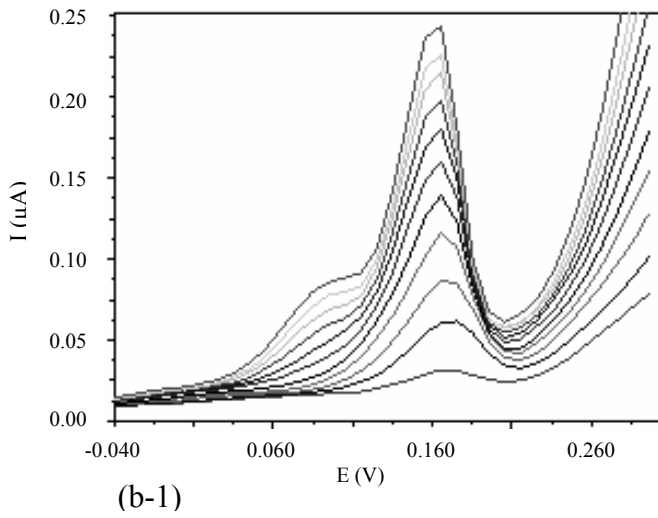
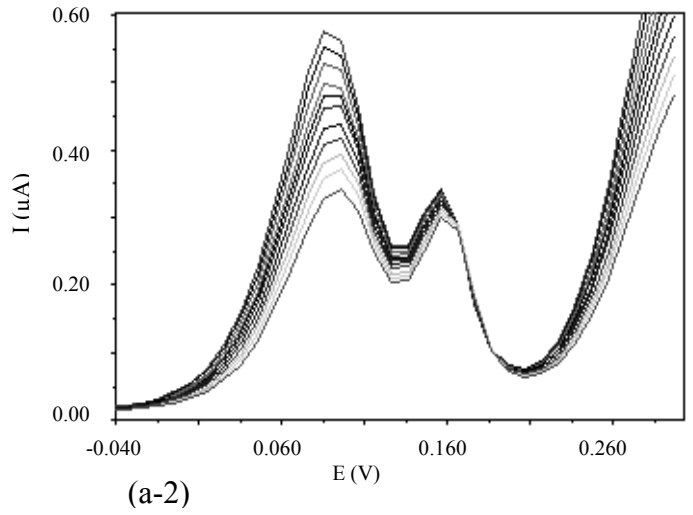
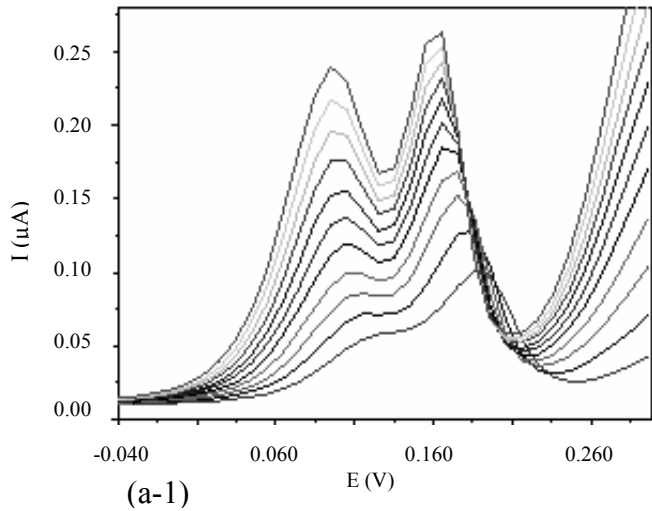


Figure 3. Titration graphs for wine in day 1 of fermentation. (a): $i_{\text{peak 1}}$ belonging to the less anodic signal (ca. 0.090 V); (b): $i_{\text{peak 2}}$ belonging to the more anodic potential (ca. 0.160 V).

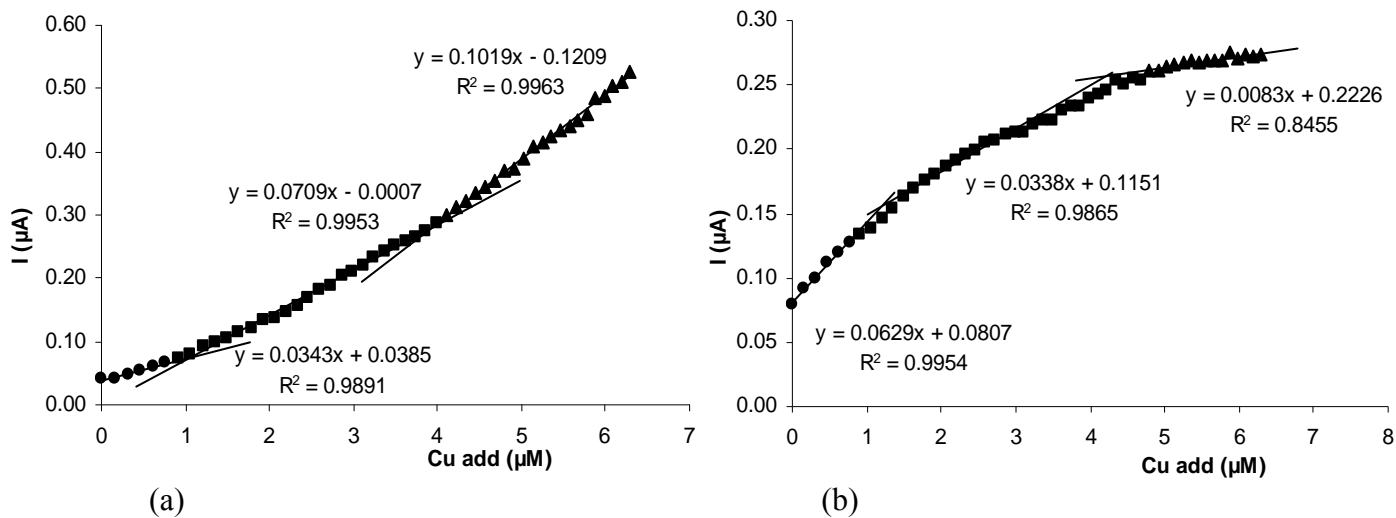


Figure 4. Langmuir (a) and Scatchard (b) linearized data from Cu-titrated wine under vinification (day 1). $[\text{Cu}']$: free metal concentration in solution; $[\text{CuL}]$: complexed copper concentration.

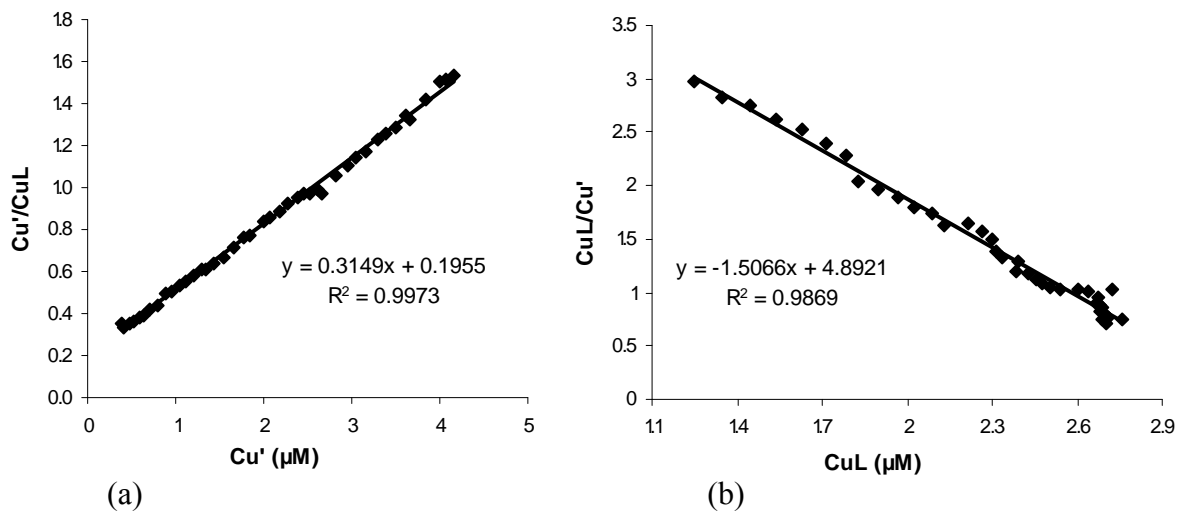


Figure 5. Molecular structures of studied cyanidin forms. (1): carbinol; (2): chalcone

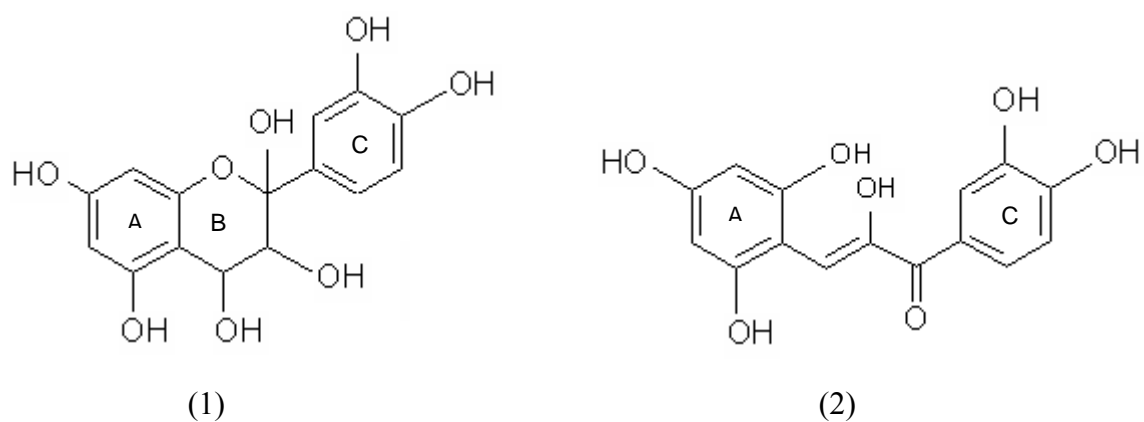


Figure 6. Binding interaction between cyanidin (bended carbinol form) and Cu (metallic divalent ion surrounded by six water molecules) depicting (in the right picture) total charge density on Cu for this interaction.

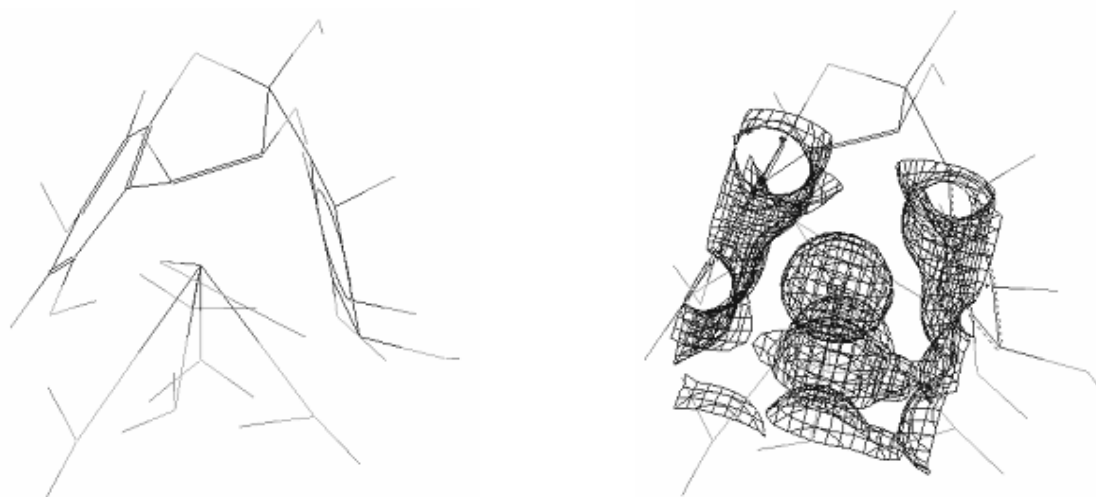


Figure 7. Most favourable binding interactions between cyanidin (chalcone trans-isomer form) and Cu (divalent species solvated by six molecules of water) showing (right sides of pictures) total charge density on Cu for these interactions.

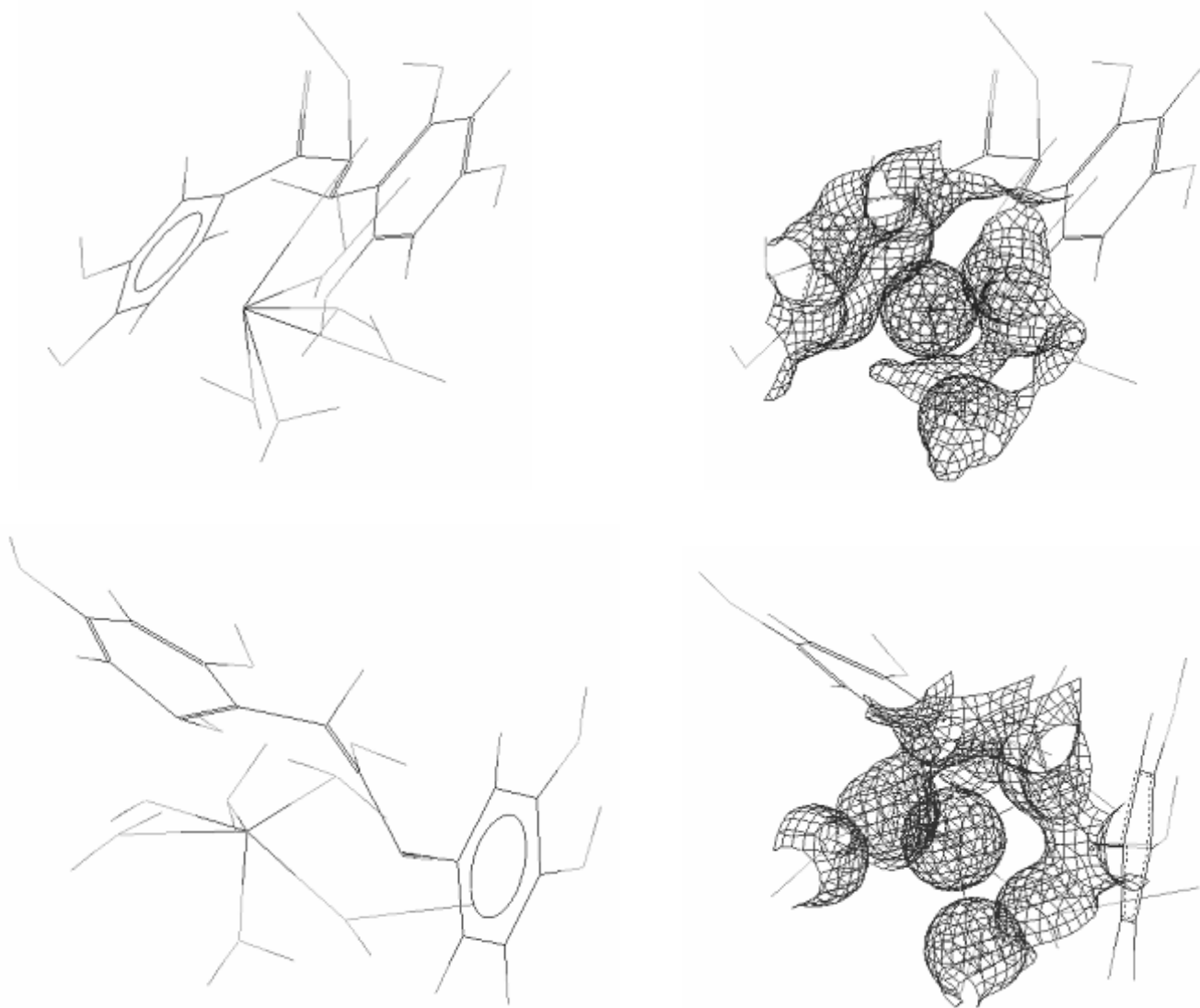


Table 1. Total complexing ligand concentration (L_T) and weak dissociable conditional formation constants (K'_{Zn}) as evaluated from Langmuir and Scatchard algorithms for Zn, obtained from wines under vinification and from commercial wines.

	Total Zn (mg/L)	LANGMUIR		SCATCHARD	
		L_T (μ M)	$K'_{Zn} \times 10^{-6}$ (M^{-1})	L_T (μ M)	$K'_{Zn} \times 10^{-6}$ (M^{-1})
<i>FERMENTATION PROCESS</i>					
Day 1	0.446 ± 0.009	0.330 ± 0.033	2.594 ± 2.164		
Day 2	0.295 ± 0.007	0.571 ± 0.024	1.114 ± 0.175	0.599 ± 0.155	0.954 ± 0.144
Day 3	0.256 ± 0.009	2.633 ± 0.197	0.228 ± 0.024	2.754 ± 0.946	0.214 ± 0.023
Day 4	0.230 ± 0.008	0.713 ± 0.041	0.753 ± 0.117	0.729 ± 0.162	0.734 ± 0.148
Day 5	0.201 ± 0.008	1.021 ± 0.060	0.805 ± 0.125	1.052 ± 0.151	0.773 ± 0.128
Day 6	0.531 ± 0.030	1.515 ± 0.046	0.713 ± 0.051	1.505 ± 0.134	0.726 ± 0.046
Day 7	0.337 ± 0.006	3.478 ± 0.118	0.492 ± 0.027	3.455 ± 0.120	0.498 ± 0.025
Day 8	0.270 ± 0.006	1.439 ± 0.053	0.586 ± 0.050	1.488 ± 0.052	0.548 ± 0.041
Day 9	0.225 ± 0.009	1.535 ± 0.027	0.970 ± 0.049	1.569 ± 0.064	0.923 ± 0.036
Day 32	0.233 ± 0.012	3.404 ± 0.700	0.209 ± 0.063	3.524 ± 1.050	0.204 ± 0.062
<i>COMMERCIAL WINES</i>					
N1	0.768 ± 0.005	2.615 ± 0.043	0.649 ± 0.025	2.626 ± 0.092	0.644 ± 0.026
N2	0.752 ± 0.007	1.107 ± 0.035	3.376 ± 1.037	1.539 ± 0.115	1.018 ± 0.076
N3	1.055 ± 0.008	2.434 ± 0.051	0.683 ± 0.038	2.492 ± 0.131	0.647 ± 0.031
N4	0.875 ± 0.008	2.089 ± 0.069	0.759 ± 0.067	2.067 ± 0.183	0.773 ± 0.067
N5	0.495 ± 0.003	2.320 ± 0.088	0.589 ± 0.049	2.509 ± 0.165	0.510 ± 0.031
N6	0.393 ± 0.003	1.156 ± 0.127	0.679 ± 0.192	1.255 ± 0.490	0.592 ± 0.393
R1	0.415 ± 0.008	3.918 ± 0.251	0.315 ± 0.029	4.049 ± 0.349	0.302 ± 0.030
R2	0.727 ± 0.009	1.453 ± 0.026	2.291 ± 0.257	1.554 ± 0.093	1.704 ± 0.115

Table 2: Total complexing ligand concentration (L_T) and weak dissociable conditional formation constants (K'_{Cu}) as evaluated from Langmuir and Scatchard algorithms for Cu, obtained from wines under vinification and from commercial wines.

	Total Cu (mg/L)	LANGMUIR		SCATCHARD	
		L_T (μ M)	$K'_{Cu} \times 10^{-6}$ (M^{-1})	L_T (μ M)	$K'_{Cu} \times 10^{-6}$ (M^{-1})
<i>FERMENTATION PROCESS</i>					
Day 1	0.958 ± 0.122	3.176 ± 0.026	1.611 ± 0.064	3.247 ± 0.047	1.507 ± 0.029
Day 2	0.432 ± 0.004	2.631 ± 0.034	1.321 ± 0.079	2.555 ± 0.092	1.503 ± 0.066
Day 3	0.290 ± 0.007	4.155 ± 0.053	1.182 ± 0.050	4.073 ± 0.123	1.260 ± 0.053
Day 4	0.207 ± 0.003	1.976 ± 0.011	3.535 ± 0.213	1.980 ± 0.082	3.475 ± 0.161
Day 5	0.170 ± 0.006	2.298 ± 0.016	2.602 ± 0.151	2.283 ± 0.087	2.746 ± 0.121
Day 6	0.180 ± 0.005	3.598 ± 0.050	1.802 ± 0.110	3.548 ± 0.141	1.890 ± 0.098
Day 7	0.167 ± 0.010	2.689 ± 0.023	1.553 ± 0.067	2.662 ± 0.067	1.629 ± 0.050
Day 8	0.178 ± 0.007	2.364 ± 0.025	1.689 ± 0.102	2.357 ± 0.081	1.726 ± 0.071
Day 9	0.202 ± 0.009	2.293 ± 0.021	1.829 ± 0.100	2.304 ± 0.069	1.786 ± 0.064
Day 10	0.190 ± 0.004	1.800 ± 0.016	2.138 ± 0.124	1.806 ± 0.065	2.103 ± 0.087
Day 18	0.131 ± 0.007	1.389 ± 0.015	2.041 ± 0.169	1.394 ± 0.066	2.004 ± 0.100
Day 32	0.158 ± 0.008	1.649 ± 0.027	1.629 ± 0.128	1.657 ± 0.083	1.605 ± 0.090
Day 58	0.083 ± 0.009	1.298 ± 0.023	1.602 ± 0.145	1.309 ± 0.111	1.663 ± 0.145
<i>COMMERCIAL WINES</i>					
N1	$0,113 \pm 0,004$	1.340 ± 0.037	0.649 ± 0.055	1.296 ± 0.285	0.588 ± 0.056
N2	$0,049 \pm 0,003$	0.636 ± 0.015	1.273 ± 0.109	0.627 ± 0.084	1.349 ± 0.088
N3	$0,157 \pm 0,003$	0.587 ± 0.019	1.812 ± 0.330	0.589 ± 0.088	1.804 ± 0.157
N4	$0,117 \pm 0,007$	0.795 ± 0.015	3.910 ± 0.476	0.773 ± 0.035	4.629 ± 0.239
N5	$0,037 \pm 0,002$	1.894 ± 0.057	0.478 ± 0.035	1.897 ± 0.168	0.482 ± 0.024
N6	$0,166 \pm 0,003$	3.208 ± 0.074	0.373 ± 0.017	3.112 ± 0.150	0.396 ± 0.017
R1	$0,084 \pm 0,006$	0.650 ± 0.030	1.370 ± 0.248	0.683 ± 0.115	1.340 ± 0.117
R2	$0,053 \pm 0,004$	1.146 ± 0.030	0.468 ± 0.031	1.199 ± 0.424	0.421 ± 0.041